Journal of the American Heart Association

ORIGINAL RESEARCH

Cardioprotective Actions of a Glucagon-like Peptide-1 Receptor Agonist on Hearts Donated After Circulatory Death

Sachiko Kadowaki, MD, PhD; M. Ahsan Siraj, MBBS, PhD; Weiden Chen, MD, PhD; Jian Wang, CPC, CCP; Marlee Parker, CPC, CCP; Anita Nagy, MD; Chun-Po Steve Fan, PhD, P.Stat; Kyle Runeckles, MSc; Jing Li, MD, PhD; Junko Kobayashi, MD, PhD; Christoph Haller, MD; Mansoor Husain, MD; Osami Honjo, MD, PhD

BACKGROUND: Heart transplantation with a donation after circulatory death (DCD) heart is complicated by substantial organ ischemia and ischemia–reperfusion injury. Exenatide, a glucagon-like peptide–1 receptor agonist, manifests protection against cardiac ischemia–reperfusion injury in other settings. Here we evaluate the effects of exenatide on DCD hearts in juvenile pigs.

METHODS AND RESULTS: DCD hearts with 15-minutes of global warm ischemia after circulatory arrest were reperfused ex vivo and switched to working mode. Treatment with concentration 5-nmol exenatide was given during reperfusion. DCD hearts treated with exenatide showed higher myocardial oxygen consumption (exenatide [n=7] versus controls [n=7], over 60–120 minutes of reperfusion, $P<0.001$) and lower cardiac troponin-I release (27.94±11.17 versus 42.25±11.80 mmol/L, $P=0.04$) during reperfusion compared with controls. In working mode, exenatide-treated hearts showed better diastolic function (dp/dt min: −3644±620 versus −2193±610 mmHg/s, $P<0.001$; Tau: 15.62±1.78 versus 24.59±7.35 milliseconds, $P=0.02$; lateral e' velocity: 11.27 ± 1.46 versus 7.19±2.96, $P=0.01$), as well as lower venous lactate levels (3.17±0.75 versus 5.17±1.44 mmol/L, $P=0.01$) compared with controls. Higher levels of activated endothelial nitric oxide synthase (phosphorylated to total endothelial nitric oxide synthase levels: 2.71±1.16 versus 1.37±0.35, $P=0.02$) with less histological evidence of endothelial damage (von Willebrand factor expression: 0.024±0.007 versus 0.331±0.302, pixel/μm, $P=0.04$) was also observed with exenatide treatment versus controls.

CONCLUSIONS: Acute treatment of DCD hearts with exenatide limits myocardial and endothelial injury and improves donor cardiac function.

Key Words: donation after circulatory death heart ■ glucagon-like peptide-1 ■ ischemia reperfusion injury ■ pediatric heart transplantation ■ pig

Donation after circulatory death (DCD) has potential to expand the donor pool for patients awaiting heart transplantation. Recent reports showed reassuring short and midterm results of DCD heart transplantation in adults that were comparable to those of heart transplantation using donation after brain death hearts.[1,2] Evolution of DCD heart transplantation has been supported by a commercially available ex-vivo heart perfusion (EVHP) device, Organ Care System (OCS, TransMedics, Inc., MA), which enables DCD hearts to be reperfused under resting conditions, minimizing ischemic periods, and rehabilitation before transplantation. However, OCS is designed for adult-size heart donors, which excludes the majority of potential pediatric heart donors. In a report of pediatric DCD heart transplantation

Correspondence to: Osami Honjo, MD, PhD, Division of Cardiovascular Surgery, Labatt Family Heart Centre, The Hospital for Sick Children, 555 University Ave, Toronto, Ontario M5G 1X8, Canada. Email: osami.honjo@sickkids.ca

Supplemental Material is available at https://www.ahajournals.org/doi/suppl/10.1161/JAHA.122.027163

For Sources of Funding and Disclosures, see page 12.

JAHA is available at: www.ahajournals.org/journal/jaha

CLINICAL PERSPECTIVE

What Is New?

- In a new juvenile pig model of heart donation after circulatory death, treatment with the glucagon-like peptide-1 receptor agonist exenatide regulated myocardial oxygen consumption during reperfusion and reduced myocardial injury compared with untreated controls.
- In working mode, exenatide-treated hearts donated after circulatory death demonstrated superior diastolic function with lower venous lactate levels compared with untreated controls, as well as higher levels of activated endothelial nitric oxide synthase and marked reductions in endothelial injury.

What Are the Clinical Implications?

- Acute treatment of juvenile hearts donated after circulatory death with a glucagon-like peptide-1 receptor agonist can enhance functional recovery of myocardium by reducing antecedent ischemia–reperfusion injury and potentially increase donor organ availability for children on the waiting list for heart transplantation.

Nonstandard Abbreviations and Acronyms

cTnI	cardiac troponin-I
DCD	donation after circulatory death
eNOS	endothelial nitric oxide synthase
EVHP	ex-vivo heart perfusion
GLP-1	glucagon-like peptide-1
GLP-1R	glucagon-like peptide-1 receptor
HR	heart rate
IRI	ischemia–reperfusion injury
MVO_2	myocardial oxygen consumption
p-eNOS	phospho-endothelial nitric oxide synthase
TUNEL	terminal deoxynucleotidyl transferase biotin-dUTP nick end labeling
vWF	von Willebrand factor

using OCS, mean body weight of heart donors was 63±11 kg.[3]

Mortality for children on the cardiac transplant waiting list is the highest among all of transplant medicine, reported as ≈25% in infants and ≈15% in children and adolescents.[4,5] In addition to the substantial warm ischemia and subsequent ischemia reperfusion injury (IRI) of DCD hearts,[6] children requiring heart transplantation often have multiple independent risk factors that increase waitlist mortality, including low body weight, high incidence of congenital heart disease, and requirement of extracorporeal membrane oxygenation.[5,7] Given the above, pediatric-size EVHP devices and therapeutic agents for pediatric DCD hearts are pressing unmet clinical needs.

The initial process of causing myocardial injury on DCD hearts is triggered by anaerobic metabolism because of global warm ischemia, which depletes adenosine triphosphate stores, leading to malfunction of sodium-potassium adenosine triphosphatase and intracellular acidosis.[8] Although subsequent reperfusion normalizes extracellular pH through sodium-hydrogen exchange,[8,9] this drives intracellular calcium overload via sodium-calcium exchange, which triggers opening of the mitochondrial permeability transition pore and subsequent activation of apoptosis.[8–10] Glucagon-like peptide-1 (GLP-1) receptor agonists represent a potential therapeutic approach to inhibiting IRI via multiple mechanisms. GLP-1 is an incretin hormone secreted by intestinal L-cells in response to feeding. Native GLP-1(7–36) is rapidly degraded by dipeptidyl peptidase-4 and neutral endopeptidase to GLP-1(9–36), GLP-1(28–36), and GLP-1(32–36).[11,12] GLP-1 mediates glucoregulatory effects by binding to its receptor (GLP-1R). The degradation-resistant GLP-1R agonist exenatide was approved as an antidiabetic drug for adults by the United States Food and Drug Administration in 2005[13,14] and for children aged 10 to 17 years in 2021.[15] GLP-1R-agonists including exenatide, native GLP-1, and its metabolites have demonstrated cardioprotective effects in animals and humans.[16–19] Several potential mechanisms for these benefits have been reported, in addition to increasing myocardial glucose uptake.[20] In an in-vitro model of cardiomyocyte hypoxia/reoxygenation, exenatide improved mitochondrial function by inhibiting calcium overload and opening mitochondrial permeability transition pores, as well as enhancing adenosine triphosphate synthesis and the activity of sodium-potassium adenosine triphosphatase through the GLP-1R/3′,5′-cyclic adenosine monophosphate/protein kinase A signaling pathway.[21] Another study showed that exenatide attenuates endothelial dysfunction and activates survival kinases to mitigate IRI.[22] Here we sought to elucidate the effects of exenatide in a juvenile pig DCD heart model using a pediatric-specific EVHP.[23]

METHODS

The data that support the findings of this study are available from the corresponding author upon reasonable request.

Study Design

All experiments were performed in accordance with a protocol approved by the Animal Care Committee of the Hospital for Sick Children, in which sample-size and

power calculation were reviewed. Fourteen Yorkshire pigs (10–12 kg, age 4 months, Lifetime Solutions Ltd., ON, Canada) were used as heart donors with a blood donor pig (20 kg, age 8 months, Lifetime Solutions Ltd., ON, Canada) for each. Harvested DCD hearts were allocated into 2 groups: untreated control group (n=7) and the exenatide treatment group (5 nmol/L, Bachem, CA; n=7) based on a previous dose–response study.[16] The EVHP cannulation configuration is shown in Figure 1A. Exenatide was added into the venous reservoir 20 minutes before reperfusion. DCD hearts were reperfused on EVHP for 2 hours and then switched to working mode to assess cardiac function. The experimental protocol is shown in Figure 1B.

DCD Heart Model

All pigs were premedicated with ketamine (10 mg/kg), atropine (0.015 mg/kg), and acepromazine (0.2 mg/kg) intramuscularly before endotracheal intubation.[23] General anesthesia was maintained by 2% isoflurane inhalation with oxygen. After a median sternotomy, baseline assessment of the cardiac function was performed. A 16-G cannula was inserted into the

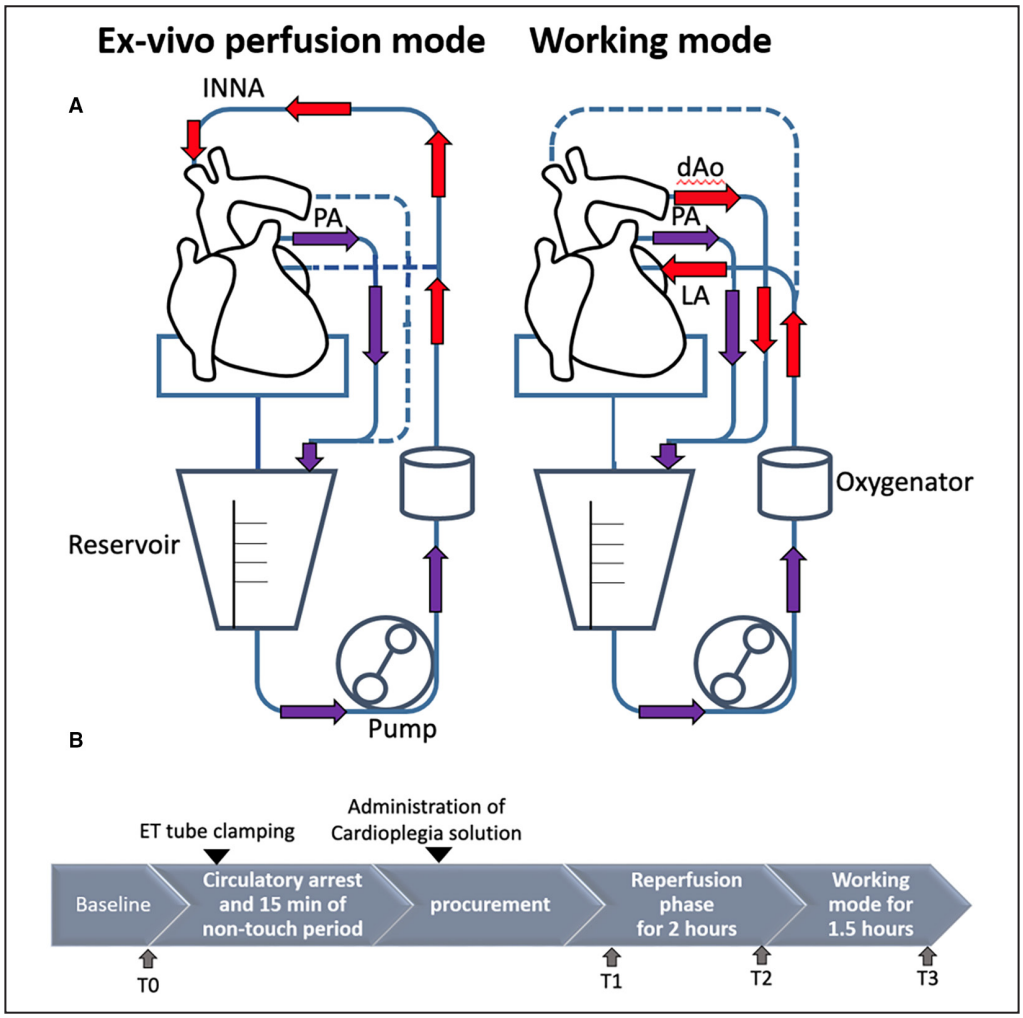

Figure 1. Perfusion methods and experimental protocol.
All donations after circulatory death (DCD) hearts were reperfused on the EVHP for 2 hours, and then switched to the working mode to assess functional recovery. During the working mode, DCD hearts were preloaded and allowed to eject 120% of cardiac output. **A**, Ex-vivo perfusion mode (left) and working mode (right) are shown. Dotted lines indicate clamped and not used. Arrows show flow directions and red and purple indicate arterial and venous blood, respectively. **B**, Experimental protocol. Circulatory arrest was induced via clamping an endotracheal tube, and then DCD hearts were procured after 15 minutes of nontouch period. Exenatide was added into the ex-vivo heart perfusion circuit 20 minutes before reperfusion in the treatment group to get uniform concentration in the perfusate. There are 4 designated time points to get blood samples: T0, before ischemia; T1, immediate after reperfusion; T2, 2 hours after reperfusion; and T3, at the end of the working mode. dAo indicates descending aorta; ET, endotracheal tube; EVHP, ex-vivo heart perfusion; INNA, innominate artery; LA, left atrium; and PA, pulmonary artery.

aortic root for cardioplegia administration, and heparin (1000 U/kg) was given through the cannula.[23] The ventilation was discontinued, and circulatory arrest was declared when no pulsation was seen on the arterial pressure waveform. Subsequently, the heart was left at rest for 15 minutes, as the assumed total duration of 5 minutes of standoff time and 10 minutes of sternotomy in the clinical setting of DCD hearts.[23] Then, 500 mL of cardioplegia solution (34.95 mL of dextrose 70%, 5 mL of KCl 2 mmol/L, 3.37 mL of NaCl 4 mmol/L, 0.38 mL of Mg_2SO_4 2 mmol/L, 456.30 mL of water, supplemented with 1000 U of erythropoietin, and 50 mg of nitroglycerin[24]) was administered into the coronary arteries via the aortic root while decompressing both ventricles by transecting the inferior vena cava and right lower pulmonary vein immediately before delivery of the cardioplegia solution. Warm ischemic time was introduced via mechanical ventilation withdrawal until cardioplegia infusion.

Ex-Vivo Heart Perfusion

Perfusate composition is shown in Table S1. After the completion of cardioplegia infusion, the heart was procured and weighed. Cannulas were inserted into the innominate artery and the descending aorta, which were then connected to the EVHP system (Figure 1A).[23] The heart was reperfused through the cannula inserted into the innominate artery with a flow rate of 10 mL/kg per min at 36.5 °C, which is defined based on physiological coronary flow as 10% of estimated cardiac output, following a flow-targeted strategy.[23] The descending aortic cannula was clamped after de-airing at the beginning of reperfusion. After initiating reperfusion, a cannula was inserted into the main pulmonary artery to drain the coronary effluent. The superior- and inferior-vena cava were oversewn. A ventricular pacing wire was placed for ventricular pacing if heart rate (HR) fell <120 beats per minute, which never occurred. Continuous epinephrine infusion at 0.05 μg/kg per minute was commenced 20 minutes after reperfusion, and then was increased to 0.10 μg/kg per minute 10 minutes before changing to working mode.[23] Body weight of each heart donor pig was used to calculate dose of epinephrine. Another arterial cannula, pressure line, and vent tube were inserted into the left atrium before switching to working mode. During reperfusion phase, coronary perfusion pressure, coronary artery flow, pulmonary arterial flow, HR, and temperature of the circuit were continuously monitored.

Working Mode

After reperfusion phase, the perfusion configuration was transitioned to working mode, in which the left atrium was filled with perfusate by the pump, while the arterial cannula at the innominate artery was clamped (Figure 1A).[23] Afterload of coronary perfusion was maintained by partially occluding the descending aortic cannula. Preload was gradually increased up to 120% of estimated cardiac output. The heart was kept in working mode for 1.5 hours (90 minutes) to assess cardiac function.

Assessments of Cardiac Function

Hemodynamic function was assessed before ischemia as a baseline and in working mode. Echocardiography was performed with a Vivid S6 ultrasound transducer (GE Healthcare, IL). Left ventricular ejection fraction was measured by the modified Simpson method. Peak early diastolic tissue velocity was measured at the lateral and septal mitral annulus from tissue Doppler in the apical 4-chamber view.

A pressure-volume catheter (VSL, Transonic Inc., STATE) connected to an ADV500 Combo PV Foundation System (version 5.0; Transonic Inc., STATE) was inserted into the left ventricle (LV) through the apex. Data obtained at baseline before ischemia and during working mode were analyzed by LabChart 8 (ADInstruments Inc., CO).

Metabolic Variables and Myocardial Injury

Arterial blood was obtained from an arterial line postoxygenator. Venous blood was collected from the coronary sinus via a cannula in the pulmonary artery. Both arterial and venous blood sampling were performed every 30 minutes during reperfusion and working mode. At each time point, blood gas analysis was performed with an iSTAT analyzer (Abbott Inc., IL) to calculate venoarterial lactate difference, myocardial oxygen consumption (MVO_2), arterial oxygen content, venous oxygen content, and coronary vascular resistance. Formulas to calculate these parameters are provided in Supplemental Materials. Arterial blood was collected at 4 time points: before ischemia as baseline (T0), immediately after initiation of reperfusion (T1), 2 hours after reperfusion (T2), and 90 minutes after working mode (T3). Collected blood was centrifuged at 4 °C, 1000*g* for 15 minutes to obtain plasma, in which cardiac troponin-I (cTnI) was measured by high sensitivity pig cTnI enzyme-linked immunosorbent assay (Life Diagnostics Inc., PA) in a blinded fashion. Hearts were weighed after harvest and after T3 to calculate heart weight gain rate (net increase of heart weight divided by heart weight after ischemia).

Western Blot

Myocardial tissue samples were obtained from the right ventricle free wall at T3 and flash frozen at −80 °C. Whole tissue was homogenized, after which protein extraction and quantification was performed using Tissue Extraction Reagent-I and Protease and

Phosphatase Inhibitor EDTA-Free (ThermoFisher, MA). Next, 30 μg of each tissue protein extract was loaded on SDS-PAGE with running buffer (10× Tris/Glycine/SDS, Bio-Rad, ON), blotted on a polyvinylidene difluoride membrane with 10× Tris/Glycine buffer (Bio-Rad, ON), and probed overnight at 4 °C for cleaved caspase–3 (#9661, 1:1000), Akt (#4691, 1:1000), phospho-Akt (#4060, 1:2000), endothelial nitric oxide synthase (eNOS; #32027, 1:1000), phospho-eNOS (#9570, 1:1000; all Cell Signaling, MA) and GAPDH (G8795, 1:15000, Sigma-Aldrich, MO) as loading control. Protein bands were detected using corresponding horseradish peroxidase–conjugated goat anti-mouse (#7076, 1:3000) or anti-rabbit secondary antibodies (#7074, 1:1000; both Cell Signaling), imaged via chemiluminescence on an Odyssey Fc Imaging System and quantified using Imaging Studio ver. 5.0 (LI-COR Biotechnology, NE).

Histopathology

Whole hearts were fixed in 10% buffered formalin at the end of each experiment, and sectioned transversely at midventricle, with samples taken from the anterior to lateral free LV wall for histological assessment. These were paraffin-embedded, sectioned at 4 μm, and stained with H&E, and immunohistochemistry for von Willebrand factor (vWF). H&E-stained sections were quantitatively scored in a blinded fashion by a pathologist. The extent of myocardial hemorrhaging on each section was scored as 0 (none), 1 (<10%), 2 (10%–50%), or 3 (>50%), with endocardial and epicardial hemorrhage also scored as 0 (none), 1 (<5%), 2 (5%–10%), or 3 (>10%). Contraction bands and/or hypereosinophilic myocytes were also assessed as 0 (absent), 1 (present). Staining for vWF was used as a marker for endothelial cell injury. After deparaffinization and rehydration, antigen retrieval (Dako Target Retrieval Solution, pH9, Agilent) was performed for subsequent probing with an anti-vWF antibody (GA527, 1:400, Dako). An anti-rabbit secondary antibody (VECTASTAIN Elite ABC-Peroxidase kit, Vector Laboratories) and 3,3′-diaminobenzidine (SigmaFAST DAB, Sigma-Aldrich) were used for detection and staining. Hematoxylin was used for counterstaining. vWF density was expressed as a pixel unit and calibrated by the sum of inner perimeters of vessels in each section using Adobe Photoshop 2020 (Adobe, CA). The same threshold density for vWF-positive staining was applied to all sections. To assess apoptosis, a TUNEL (terminal deoxynucleotidyl transferase biotin-dUTP nick end labeling) assay was performed as per manufacturer's instructions (ApopTag Plus Fluorescein In Situ Apoptosis Detection Kit, EMD Millipore Corporation, CA), and the number of TUNEL-positive nuclei was quantified in 6 randomly picked fields/sections with an open-source digital image analysis software (QuPath v0.2.3) at 20X and averaged. TUNEL-positive nuclei were expressed as a percentage of total nuclei.

Statistical Analysis

Subject characteristics were summarized using means and SDs. Characteristics at baseline, following reperfusion, and in working mode were compared between treatment and control groups using a descriptive table, and continuous measures were additionally described with bar charts. Between-group differences in continuous variables were assessed using paired t test or Wilcoxon rank-sum tests; between-group differences in scoring results of H&E staining across groups were assessed using Fisher exact tests. Longitudinal data over the course of 2-hour reperfusion were analyzed using linear mixed-effects models with case-specific intercepts as random effects, and the significance of each variable using *F* tests. We also evaluated the overall significance of the drug effect over the course of reperfusion using χ^2 tests. A *P* value of <0.05 was considered significant. Statistical analyses used R v 3.4.1 (R Foundation for Statistical Computing, Austria).

RESULTS

There were no significant differences in the body weight of pigs in the treatment and control groups (exenatide versus controls, 11.3±0.8 versus 11.2±2.4 kg, *P*=0.93) or in duration of warm ischemic time (22±2 versus 21±2 min, *P*=0.56). All hearts regained sinus rhythm spontaneously after reperfusion or after cardioversion.

Metabolic Variables and Myocardial Injury

DCD hearts treated with exenatide showed significantly higher MVO_2 during reperfusion compared with untreated controls (*P*<0.001), but not during working mode (Figure 2A). Venous lactate levels showed no difference during reperfusion (*P*=0.75) but were significantly lower in exenatide-treated DCD hearts during working mode (3.17 ± 0.75 versus 5.17 ± 1.44 mmol/L, *P*=0.01; Figure 2B). Coronary vascular resistance did not differ between groups during either reperfusion (*P*=0.42) or working mode (*P*=0.26; Figure 2C). Regression tables of MVO_2, venous lactate level, and coronary vascular resistance are described in Table S2. Levels of cTnI were not detectable in either group at T0 or T1, but were significantly lower in exenatide-treated hearts at T2 (27.9±11.2 versus 42.3±11.8 ng/mL, *P*=0.04) and remained trending towards this at T3 (70.7±11.4 versus 88.0±17.2 ng/mL, *P*=0.09; Figure 3A). Heart weight gain, a measure of myocardial edema,

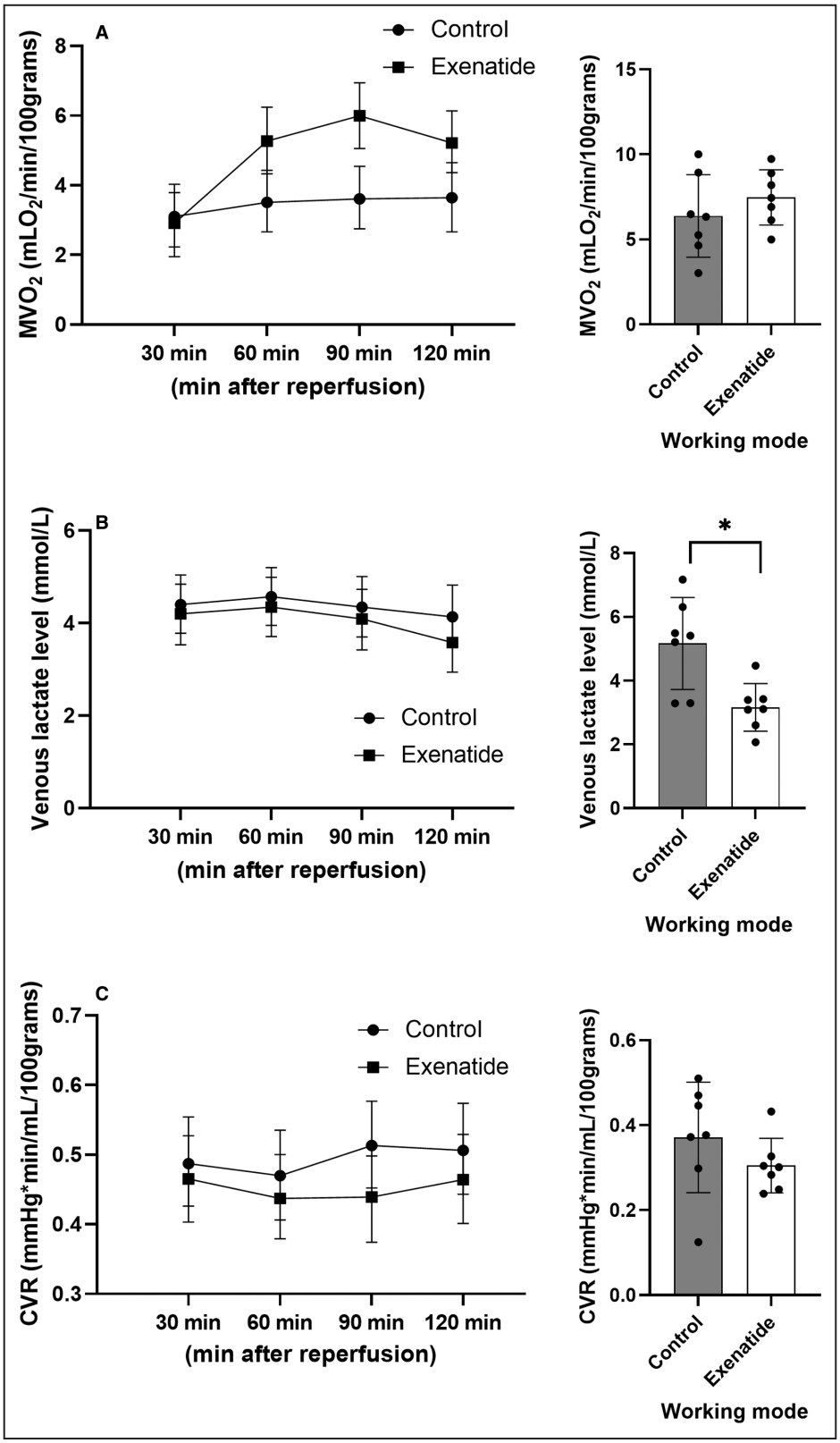

Figure 2. Metabolic markers during reperfusion and at the working mode.
A, Myocardial oxygen consumption ($P<0.001$ over the 2-hour reperfusion); **B**, venous lactate level; **C**, coronary vascular resistance. An error bar represents the average response and its corresponding 95% CI at each time point for each group during reperfusion. Data represent the mean±SD in working mode. *$P<0.05$ in working mode. CVR indicates coronary vascular resistance; and MVO_2, myocardial oxygen consumption.

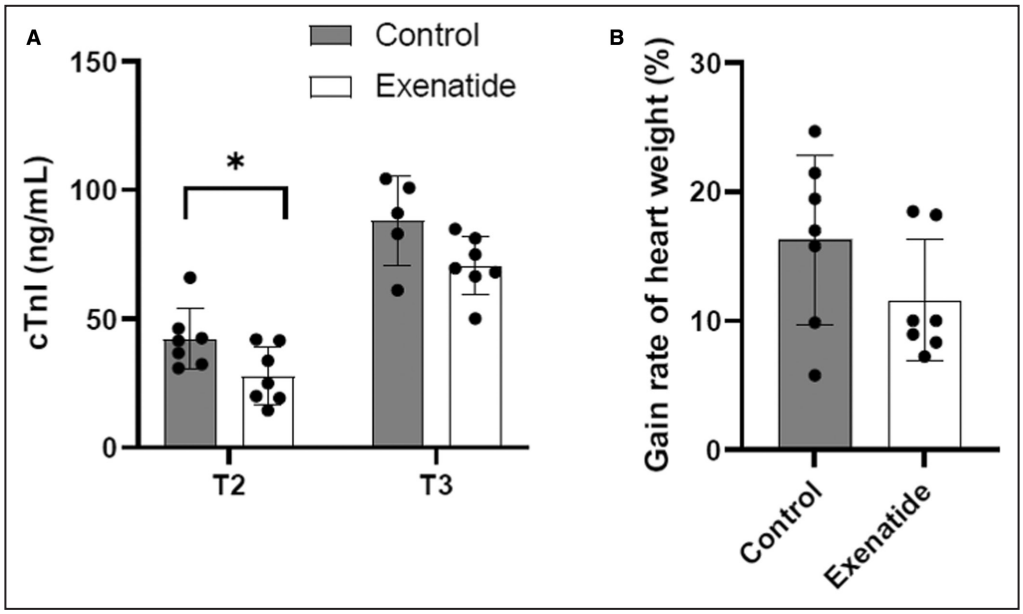

Figure 3. Myocardial damage markers.
A, Cardiac troponin I level measured at T2 and T3; **B**, heart weight gain rate at the end of working mode relative to the weight of procured heart after ischemia. *P<0.05. cTnI indicates cardiac troponin I.

did not differ between the 2 groups (11.6±4.7 versus 16.3±6.6, %, P=0.15; Figure 3B).

Cardiac Function

Functional parameters determined by pressure-volume catheter and echocardiogram are shown in Table 1. Treatment with exenatide improved diastolic function as compared with controls: minimum first derivative of LV pressure (Min-dp/dt: −3644 ± 620 versus −2193 ± 610 mm Hg/s, P<0.001), Tau (15.6±1.8 versus 24.6±7.4 ms, P=0.02), and lateral peak early diastolic tissue velocity (11.3±1.5 versus 7.2±3.0 cm/s, P=0.01; Figure 4). Improvements in systolic function, as represented by maximum first derivative of LV pressure (Max +dp/dt: 2317±300 versus 1949±664 mm Hg/s, P=0.22), left ventricular ejection fraction by pressure-volume loops (46±13 versus 33%±9%, P=0.05), and by echocardiography (60±8 versus 43%±21%, P=0.08), failed to reach statistical significance (Figure 4). Of note, HR was higher in exenatide-treated hearts during working mode (201±22 versus 167±18 beats per minute, P=0.01), with no differences in stroke volume, cardiac index, and stroke work, under the same preload conditions.

Biochemical Markers

Representative Western blots for eNOS, survival kinase, and an apoptosis marker are shown in Figure 5. Treatment with exenatide increased p-eNOS/eNOS ratio compared with untreated controls (2.71±1.16 versus 1.37±0.35, P=0.02) with no differences in p-Akt/t-Akt (0.48±0.23 versus 0.45±0.13, P=0.72) or cleaved caspase-3/GAPDH (0.023±0.009 versus 0.034±0.016, P=0.15).

Histological Markers

Scores for hemorrhage in each cardiac layer, contraction bands, and hypereosinophilic myocytes are summarized in Table 2. Although no significant differences were observed, contraction bands and/or hypereosinophilic myocytes occupy <5% of all sections. In TUNEL assays, the ratio of positive cells is <1% in both groups, with no significant difference (0.76±0.33 versus 0.92±0.26, %, P=0.32; Figure S1). However, treatment with exenatide clearly and convincingly reduced vWF expression (ie, endothelial cell activation) as compared with untreated controls (0.024±0.007 versus 0.331±0.302, pixel/µm, P=0.04; Figure 6).

DISCUSSION

The DCD heart model used in this study was developed to investigate pediatric DCD heart pathophysiology. Hearts during reperfusion are in a resting state and do not pump blood. They are then filled with blood during working mode to assess hemodynamic function. This model “simulates” pediatric DCD heart transplantation and represents a platform in which innovative treatments aimed at improving DCD heart viability can be tested.

Using this model, DCD hearts treated with exenatide showed less myocardial and endothelial

Table 1. Functional Parameters

Variables	Control (n=7)	Exenatide (n=7)	*P* value
Pressure-volume catheter			
Heart rate, bpm			
Baseline	108±10	111±13	0.71
Working mode	167±18	201±22	0.01
Ejection fraction, %			
Baseline	38±5	40±3	0.49
Working mode	33±9	46±13	0.05
Max+dp/dt, mmHg/s			
Baseline	1337±426	1044±273	0.16
Working mode	1949±664	2317±300	0.22
Min-dp/dt, mmHg/s			
Baseline	−1606±511	−1333±143	0.22
Working mode	−2193±610	−3644±620	<0.001
Tau, ms			
Baseline	31.3±5.4	36.9±15	0.38
Working mode	24.6±7.4	15.6±1.8	0.02
Stroke volume, mL			
Baseline	10.5±2.3	11.3±1.5	0.46
Working mode	8.1±3.7	8.0±1.6	0.94
Cardiac index, L/min per m^2			
Baseline	2.85±0.50	3.09±0.41	0.35
Working mode	3.25±0.83	3.92±0.34	0.08
Cardiac output, mL/min			
Baseline	1151±319	1240±159	0.52
Working mode	1313±477	1578±173	0.21
Stroke work, mmHg×mL			
Baseline	634±128	614±54	0.73
Working mode	660±325	745±220	0.58
Arterial elastance, mmHg/mL			
Baseline	6.7±2.5	5.6±0.8	0.29
Working mode	14.5±5.4	14.1±2.4	0.85
Echocardiogram			
Ejection fraction, %			
Baseline	59±5	55±4	0.15
Working mode	43±21	60±8	0.08
Lateral *e′* velocity, cm/s			
Baseline	10.8±2.9	11.2±2.3	0.80
Working mode	7.2±3.0	11.3±1.5	0.01
Septal *e′* velocity, cm/s			
Baseline	7.1±1.8	5.4±1.4	0.09
Working mode*	6.9±4.4	9.8±1.9	0.18

bpm indicates beats per minute; *e′*, peak early diastolic tissue velocity; Max+dp/dt, maximum first derivative of left ventricular pressure; and Min-dp/dt, minimum first derivative of left ventricular pressure.

*n=6 in control.

damage and preserved diastolic function compared with controls. These results represent clear evidence of direct cardioprotection of the nondegradable GLP-1R agonist exenatide. Although DCD hearts treated with exenatide showed higher MVO_2 during reperfusion, suggesting greater metabolic activity, they released lower levels of the cardiac injury biomarker cTnI.

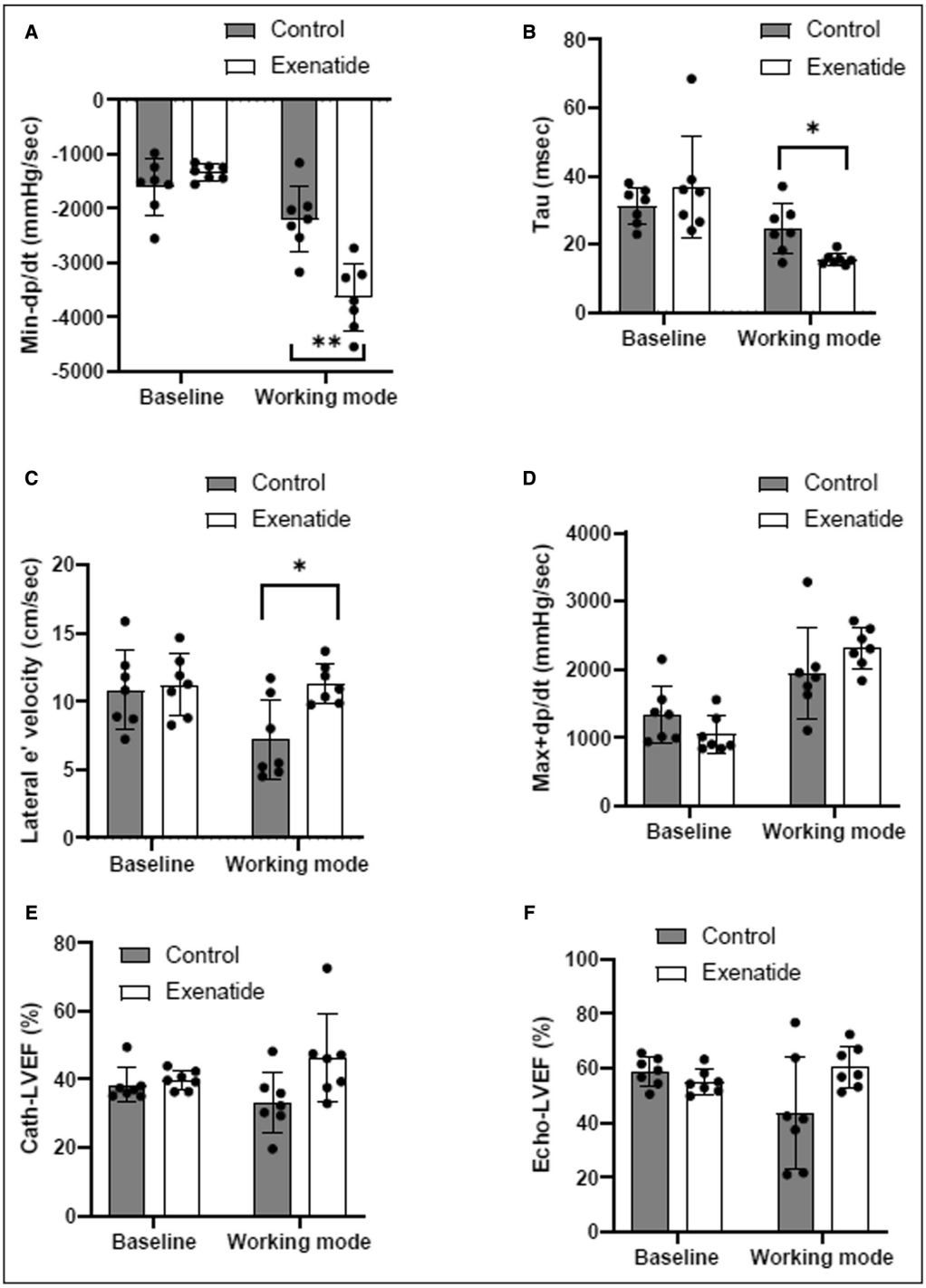

Figure 4. Parameters representing diastolic and systolic function.
A, Minimum first derivative of left ventricular pressure; **B**, Tau; **C**, lateral *e′* velocity; **D**, maximum first derivative of left ventricular pressure; **E**, left ventricular ejection fraction measured by the pressure-volume catheter; **F**, left ventricular ejection fraction measured by the echocardiogram. Data represent the mean±SD. *$P<0.05$, **$P<0.01$. Cath-LVEF indicates left ventricular ejection fraction measured by the pressure-volume catheter; Echo-LVEF, left ventricular ejection fraction measured by echocardiogram; Max+dp/dt, maximum first derivative of left ventricular pressure; and Min-dp/dt, minimum first derivative of left ventricular pressure.

Metabolic Variables

Although MVO_2 was higher in exenatide-treated DCD hearts during reperfusion, this difference disappeared in working mode. Myocardial energy (oxygen) consumption consists of 2 different components: mechanical activity (work-dependent MVO_2) and

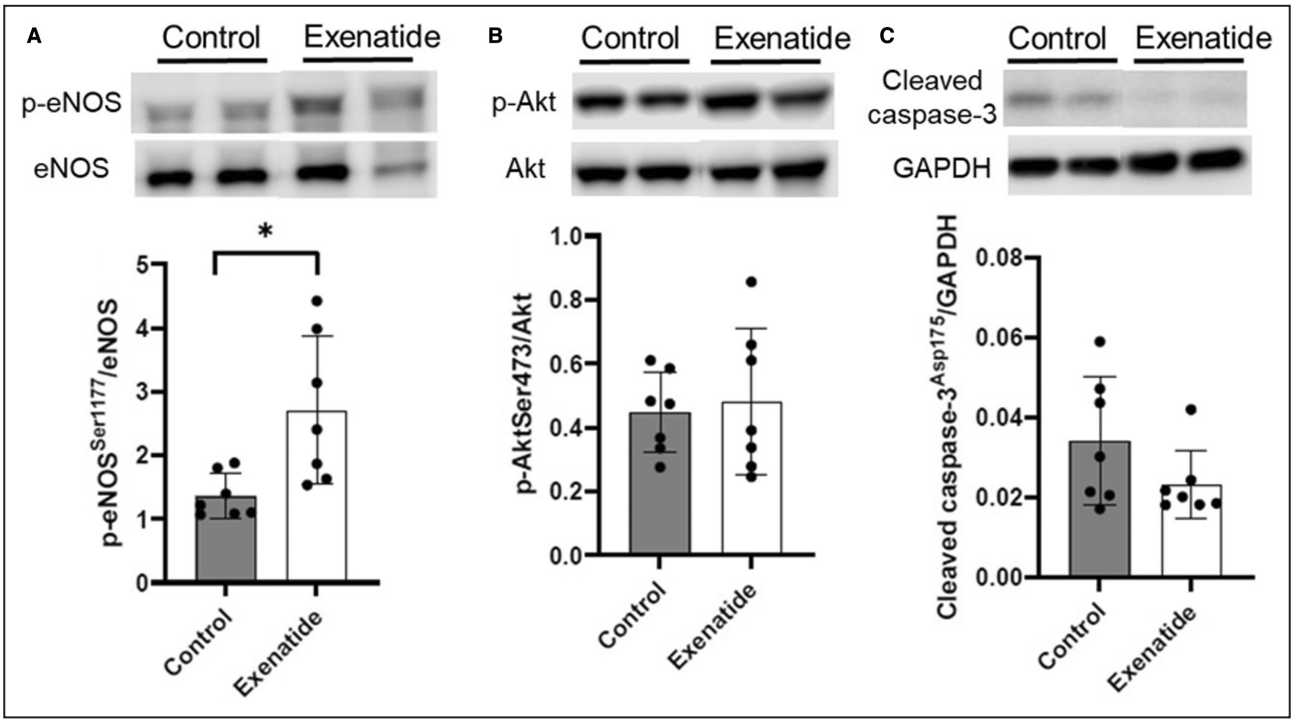

Figure 5. Western blotting.
A, Phosphorylated-endothelial nitric oxide synthase (eNOS)/eNOS assessed as endothelial function; **B**, phosphorylated-Akt/Akt assessed as antiapoptotic kinase expression; **C**, cleaved caspase-3 activation assessed as an apoptosis marker. Representative blot images are shown in each marker. Data represent the mean±SD. *P<0.05. GAPDH indicates glyceraldehyde 3-phosphate dehydrogenase; p-Akt, phosphorylated-Akt; and p-eNOS, phosphorylated-endothelial nitric oxide synthase.

nonmechanical processes (unloaded MVO_2) including maintenance of ionic environment, protein synthesis, membrane potential, and release and uptake of calcium by sarcoplasmic reticulum.[25,26] Thus, MVO_2 measured during reperfusion phase represents unloaded MVO2, and MVO2 measured in working mode is the sum of unloaded MVO2 and work-dependent MVO2. Although work-dependent MVO2 can show energy efficiency per unit of external work,[27] unloaded MVO2 reflects on the status of the myocardium and its metabolic response to recovery from ischemic- and ischemia–reperfusion injuries. Accordingly, we believe the higher unloaded MVO_2 observed in the exenatide-treated group reflects a higher proportion of myocytes functioning in the exenatide-treated DCD hearts. Importantly, the "step-up" of MVO_2 when hearts transition to working mode corresponds to work-dependent MVO_2, which was lower in exenatide-treated DCD hearts than in controls, suggesting greater energy efficiency of exenatide-treated hearts in working mode. This is further supported by the lower venous lactate levels observed in exenatide-treated DCD hearts during working mode, with less anaerobic metabolism and more oxidative phosphorylation compared with controls. Similar arterial lactate levels in the 2 groups in working mode may be explained by the EVHP circuit, in which lactate levels in the arterial line represent accumulated lactate in the venous reservoir. As such, venous lactate is a more sensitive indicator of myocardial metabolism than arterial lactate during EVHP. Taken together, our data suggest exenatide treatment better preserved myocardial metabolism in DCD hearts.

Myocardial Protection

The extent of myocardial damage in our DCD model is manifest by increased release of cTnI at T2 and T3 compared with T0, with exenatide treatment showing a 33% reduction in cTnI levels at T2 (P<0.05), and 20% lower cTnI levels at T3 (P=0.09). Cardioprotective actions of exenatide were also evidenced by higher cardiac p-eNOS/eNOS ratios. eNOS is constitutively expressed by both cardiac endothelial cells and cardiomyocytes,[28] and regulates NO-mediated vascular tone[29] and cardiac function.[30] Indeed, vasodilation through eNOS-derived NO has been shown to mediate cardioprotection against IRI.[31] Another striking manifestation of the cardioprotective actions of exenatide in DCD hearts was the extremely low level of cardiac endothelial vWF expression. This finding implicates an endothelial cell "pacification" effect of exenatide, which we previously presumed in an arterial laser injury model of thrombosis in mice.[32]

Table 2. Hematoxylin and Eosin Staining

Variables	Control (n=7)	Exenatide (n=6)	*P* value
Endocardial hemorrhage			1.00
None	0 (0%)	0 (0%)	
<5%	1 (14%)	0 (0%)	
5%–10%	2 (29%)	2 (33%)	
>10%	4 (57%)	4 (67%)	
Myocardial hemorrhage			0.07
None	2 (29%)	0 (0%)	
<10%	3 (43%)	6 (100%)	
10%–50%	2 (29%)	0 (0%)	
Epicardial hemorrhage			0.62
None	0 (0%)	2 (33%)	
<5%	4 (57%)	2 (33%)	
5%–10%	2 (29%)	1 (17%)	
>10%	1 (14%)	1 (17%)	
Contraction bands and/or hypereosinophilic myocytes			0.59
None	5 (71%)	3 (50%)	
Positive (<5%)	2 (29%)	3 (50%)	

Hemodynamic Function

Previous studies in an acute regional myocardial ischemia model in adult pigs had shown that exenatide prevented both systolic and diastolic dysfunction.[33] In the unique DCD model we have used, exenatide improved diastolic function more than systolic function. This may be because of the unique loading conditions of our model, and/or relative resistance of the ex-vivo juvenile pig heart to systolic dysfunction after IRI.[34,35] Another potential factor is the higher HR observed in the exenatide group in working mode. HR is known to affect indices of early diastolic pressure decay and cardiac contractility as well as preload and afterload. Having said that, HR alone, without changes in preload and afterload, has not shown significant impact on max+dp/dt.[36,37] Considering also that the DCD model used a strictly managed preload (120% of cardiac output in working mode) as well as a consistent afterload (as shown by arterial elastance), significant improvements in diastolic function in exenatide-treated hearts are unlikely to be caused by differences in loading, and more likely to represent direct effects on cardiac performance. With regard to the observed increase in HR in exenatide-treated DCD hearts, GLP-1 and GLP-1R agonists are known to increase HR through modulation of both autonomic nervous system activity, as well as direct effects on atrial pacemaker cells.[38–41]

Cellular Injury

Curiously, expression levels of the apoptosis marker cleaved caspase-3 and survival kinase Akt did not show significant differences between the 2 groups. This may be because of specific conditions of the DCD model. First, our model uses warm ischemic time, which did not result in irreversible cellular changes such as apoptosis. When reductions in coronary blood flow lasts longer than 20 to 40 minutes, infarction is typically observed in larger mammals.[42] Our DCD hearts underwent only 20 minutes of ischemia, rendering the myocardium on the cusp of reversible injury. The most severe manifestation of coronary microvascular injury from IRI is hemorrhage, which results from swelling of capillary endothelial cells, microvascular rupture, and leakage of circulating cells into the interstitium.[43,44] With this in mind, our blinded scoring of hemorrhage in endocardium, myocardium, and epicardium showed no differences between the 2 groups, with contraction bands and/or hypereosinophilic myocytes detected in <5% of the LV area of every section examined. Similarly, as shown by TUNEL staining, apoptotic cells represented <1% of all cells in both groups. Together, these findings indicate that while our model unequivocally manifests injury, it falls short of irreversible cell death and extensive histopathological damage.

Pediatric DCD Heart Transplantation

Understanding and minimizing IRI of DCD hearts is necessary to establish a clinically viable DCD heart transplant program. We believe the EVHP circuit we describe breaks new ground in this field, enabling DCD hearts to beat under oxygen supply and resting conditions without volume- and pressure-loading. This normothermic oxygenated perfusion minimizes myocardial ischemia time during organ transport, which is beneficial for DCD hearts showing poor tolerance of any additional cold ischemia. In addition to the pediatric-specific EVHP and optimal perfusion strategies described,[23] the current study supports the use of cardioprotective agents, such as exenatide, as a means to further minimize IRI, making available more viable DCD hearts needed to impact the excessive mortality of pediatric heart transplant waiting lists. Indeed, a preclinical pilot study using DCD hearts in pediatric patients has been approved by the Research Ethics Board of the Hospital for Sick Children. Within this protocol, donated DCD hearts are reperfused on the EVHP device, which is designed and produced for clinical use on the basis of our animal studies to date. Based on the current report, we are also well positioned to conduct first-in-human trials of cardioprotective agents, such as exenatide, on pediatric DCD hearts.

Study Limitations

We believe the warm ischemic time used in the current DCD heart model was not long enough to cause

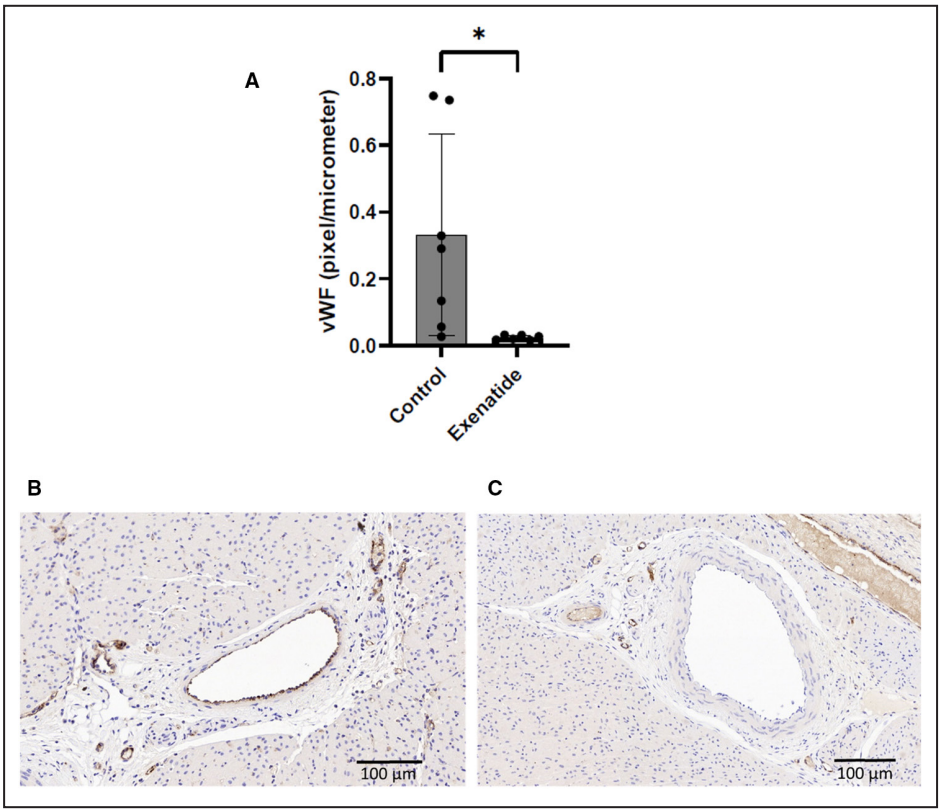

Figure 6. Expression of von Willebrand factor (vWF) in endothelial cells.
(**A**), vWF density in the control and exenatide group. Representative pictures of stained myocardium in the control and exenatide group are shown in (**B**) and (**C**), respectively. Data represent the mean±SD. *P<0.05. vWF indicates von Willebrand factor.

irreversible cardiomyocyte injury, or widespread apoptosis and cell death. As such, we were not able to demonstrate antiapoptotic effects of exenatide. We believe a longer ischemic period is required to assess those effects. Although our current model was designed to simulate current conditions of clinical practice, assessment of exenatide and other cardioprotective strategies in settings with longer durations of ischemia and more possibility for irreversible damage may be informative. This study did not use an active comparator or a blinded placebo, which would strengthen the design of future preclinical and clinical studies. Although the longitudinal analysis enabled us to gain insight into the biomarker trajectories during the reperfusion time period, the limited sample size prompts further study to confirm the longitudinal findings.

CONCLUSIONS

In a juvenile pig DCD heart model, treatment with exenatide increased MVO_2 and reduced cTnI release during reperfusion, with improved hemodynamic function and lower lactate levels in working mode compared with untreated controls. Measures of diastolic function and endothelial function also showed significant protection after treatment with exenatide. Cardioprotective strategies such as GLP-1R agonists may enhance the clinical viability of pediatric DCD heart transplantation.

ARTICLE INFORMATION

Received September 4, 2022; accepted December 9, 2022.

Affiliations

Division of Cardiovascular Surgery, The Hospital for Sick Children, Toronto, Ontario, Canada (S.K., W.C., J.L., J.K., C.H., O.H.); Department of Surgery (S.K., W.C., J.L., J.K., C.H., O.H.) and Department of Medicine, Ted Rogers Centre for Heart Research, Peter Munk Cardiac Centre (M.A.S., M.H.), University of Toronto, Toronto, Ontario, Canada; Department of Cardiac Surgery, Guangzhou Women and Children's Medical Center, Guangzhou, China (W.C.); Division of Perfusion Services (J.W., M.P.) and Division of Pathology (A.N.), The Hospital for Sick Children, Toronto, Ontario, Canada; Ted Rogers Centre for Heart Research, Peter Munk Cardiac Centre, Labatt Family Heart Centre, University Health Network, The Hospital for Sick Children, Toronto, Ontario, Canada (C-P.S.F., K.R.); Department of Cardiovascular Surgery, Okayama University Hospital, Okayama, Japan (J.K.); and Department of Cardiovascular Surgery, Faculty of Medicine, Dentistry and Pharmaceutical Sciences, Okayama University, Okayama, Japan (J.K.).

Acknowledgments

The investigators thank Dr Mark Friedberg for technical assistance for echocardiographic measurement.

Sources of Funding

This study was supported by the James H. Cummings Foundation, the Ted Rogers Centre for Heart Research Innovation Fund, and the Labatt Family Heart Centre Innovation Fund in the Hospital for Sick Children.

Disclosures

None.

Supplemental Material

Data S1
Tables S1–S2
Figure S1

REFERENCES

1. Messer S, Cernic S, Page A, Berman M, Kaul P, Colah S, Ali J, Pavlushkov E, Baxter J, Quigley R, et al. A 5-year single-center early experience of heart transplantation from donation after circulatory-determined death donors. *J Heart Lung Transplant*. 2020;39:1463–1475. doi: 10.1016/j.healun.2020.10.001
2. Dhital K, Ludhani P, Scheuer S, Connellan M, Macdonald P. DCD donations and outcomes of heart transplantation: the Australian experience. *Indian J Thorac Cardiovasc Surg*. 2020;36:224–232. doi: 10.1007/s12055-020-00998-x
3. Laurence C, Nachum E, Henwood S, Berman M, Large SR, Messer S, Kaul P, Baxter J, Quigley R, Osman M, et al. Pediatric heart transplantation following donation after circulatory death, distant procurement, and ex-situ perfusion. *J Heart Lung Transplant*. 2022;41:1104–1113. doi: 10.1016/j.healun.2022.04.013
4. Mah D, Singh TP, Thiagarajan RR, Gauvreau K, Piercey GE, Blume ED, Fynn-Thompson F, Almond CS. Incidence and risk factors for mortality in infants awaiting heart transplantation in the USA. *J Heart Lung Transplant*. 2009;28:1292–1298. doi: 10.1016/j.healun.2009.06.013
5. Zafar F, Castleberry C, Khan MS, Mehta V, Bryant R III, Lorts A, Wilmot I, Jefferies JL, Chin C, Morales DLS. Pediatric heart transplant waiting list mortality in the era of ventricular assist devices. *J Heart Lung Transplant*. 2015;34:82–88. doi: 10.1016/j.healun.2014.09.018
6. White CW, Messer SJ, Large SR, Conway J, Kim DH, Kutsogiannis DJ, Nagendran J, Freed DH. Transplantation of hearts donated after circulatory death. *Front Cardiovasc Med*. 2018;5:8. doi: 10.3389/fcvm.2018.00008
7. Rossano JW, Singh TP, Cherikh WS, Chambers DC, Harhay MO, Hayes D Jr, Hsich E, Khush KK, Meiser B, Potena L, et al. The international thoracic organ transplant registry of the International Society for Heart and Lung Transplantation: twenty-second pediatric heart transplantation report—2019; focus theme: donor and recipient size match. *J Heart Lung Transplant*. 2019;38:1028–1041. doi: 10.1016/j.healun.2019.08.002
8. Garcia-Dorado D, Ruiz-Meana M, Inserte J, Rodriguez-Sinovas A, Piper HM. Calcium-mediated cell death during myocardial reperfusion. *Cardiovasc Res*. 2012;94:168–180. doi: 10.1093/cvr/cvs116
9. Gomez L, Li B, Mewton N, Sanchez I, Piot C, Elbaz M, Ovize M. Inhibition of mitochondrial permeability transition pore opening: translation to patients. *Cardiovasc Res*. 2009;83:226–233. doi: 10.1093/cvr/cvp063
10. Sanada S, Komuro I, Kitakaze M. Pathophysiology of myocardial reperfusion injury: preconditioning, postconditioning, and translational aspects of protective measures. *Am J Physiol Heart Circ Physiol*. 2011;301:H1723–H1741. doi: 10.1152/ajpheart.00553.2011
11. Deacon CF. Circulation and degradation of GIP and GLP-1. *Horm Metab Res*. 2004;36:761–765. doi: 10.1055/s-2004-826160
12. Deacon CF, Johnsen AH, Holst JJ. Degradation of glucagon-like peptide-1 by human plasma in vitro yields an N-terminally truncated peptide that is a major endogenous metabolite in vivo. *J Clin Endocrinol Metab*. 1995;80:952–957. doi: 10.1210/jcem.80.3.7883856
13. Davidson MB, Bate G, Kirkpatrick P. Exenatide. *Nat Rev Drug Discov*. 2005;4:713–714. doi: 10.1038/nrd1828
14. Kang YM, Jung CH. Cardiovascular effects of glucagon-like peptide-1 receptor agonists. *Endocrinol Metab (Seoul)*. 2016;31:258–274. doi: 10.3803/EnM.2016.31.2.258
15. Roth CL, Perez FA, Whitlock KB, Elfers C, Yanovski JA, Shoemaker AH, Abuzzahab MJ. A phase 3 randomized clinical trial using a once-weekly glucagon-like peptide-1 receptor agonist in adolescents and young adults with hypothalamic obesity. *Diabetes Obes Metab*. 2021;23:363–373. doi: 10.1111/dom.14224
16. Ban K, Noyan-Ashraf MH, Hoefer J, Bolz SS, Drucker DJ, Husain M. Cardioprotective and vasodilatory actions of glucagon-like peptide 1 receptor are mediated through both glucagon-like peptide 1 receptor-dependent and -independent pathways. *Circulation*. 2008;117:2340–2350. doi: 10.1161/CIRCULATIONAHA.107.739938
17. Siraj MA, Mundil D, Beca S, Momen A, Shikatani EA, Afroze T, Sun X, Liu Y, Ghaffari S, Lee W, et al. Cardioprotective GLP-1 metabolite prevents ischemic cardiac injury by inhibiting mitochondrial trifunctional protein-α. *J Clin Invest*. 2020;130:1392–1404. doi: 10.1172/JCI99934
18. Nikolaidis LA, Mankad S, Sokos GG, Miske G, Shah A, Elahi D, Shannon RP. Effects of glucagon-like peptide-1 in patients with acute myocardial infarction and left ventricular dysfunction after successful reperfusion. *Circulation*. 2004;109:962–965. doi: 10.1161/01.CIR.0000120505.91348.58
19. Lønborg J, Vejlstrup N, Kelbæk H, Bøtker HE, Kim WY, Mathiasen AB, Jørgensen E, Helqvist S, Saunamäki K, Clemmensen P, et al. Exenatide reduces reperfusion injury in patients with ST-segment elevation myocardial infarction. *Eur Heart J*. 2012;33:1491–1499. doi: 10.1093/eurheartj/ehr309
20. Depre C, Ponchaut S, Deprez J, Maisin L, Hue L. Cyclic AMP suppresses the inhibition of glycolysis by alternative oxidizable substrates in the heart. *J Clin Invest*. 1998;101:390–397. doi: 10.1172/JCI1168
21. Chang G, Liu J, Qin S, Jiang Y, Zhang P, Yu H, Lu K, Zhang N, Cao L, Wang Y, et al. Cardioprotection by exenatide: a novel mechanism via improving mitochondrial function involving the GLP-1 receptor/cAMP/PKA pathway. *Int J Mol Med*. 2018;41:1693–1703. doi: 10.3892/ijmm.2017.3318
22. Wang D, Luo P, Wang Y, Li W, Wang C, Sun D, Zhang R, Su T, Ma X, Zeng C, et al. Glucagon-like peptide-1 protects against cardiac microvascular injury in diabetes via a cAMP/PKA/rho-dependent mechanism. *Diabetes*. 2013;62:1697–1708. doi: 10.2337/db12-1025
23. Kobayashi J, Luo S, Akazawa Y, Parker M, Wang J, Chiasson D, Friedberg MK, Haller C, Honjo O. Flow-targeted pediatric ex vivo heart perfusion in donation after circulatory death: a porcine model. *J Heart Lung Transplant*. 2020;39:267–277. doi: 10.1016/j.healun.2019.11.023
24. Watson AJ, Gao L, Sun L, Tsun J, Doyle A, Faddy SC, Jabbour A, Orr Y, Dhital K, Hicks M, et al. Enhanced preservation of pig cardiac allografts by combining erythropoietin with glyceryl trinitrate and zoniporide. *Am J Transplant*. 2013;13:1676–1687. doi: 10.1111/ajt.12249
25. Suga H, Hisano R, Hirata S, Hayashi T, Ninomiya I. Mechanism of higher oxygen consumption rate: pressure-loaded vs. volume-loaded heart. *Am J Physiol*. 1982;242:H942–H2948. doi: 10.1152/ajpheart.1982.242.6.H942
26. Suga H. Ventricular energetics. *Physiol Rev*. 1990;70:247–277. doi: 10.1152/physrev.1990.70.2.247
27. Suga H. Total mechanical energy of a ventricle model and cardiac oxygen consumption. *Am J Physiol*. 1979;236:H498–H505. doi: 10.1152/ajpheart.1979.236.3.H498
28. Schulz R, Nava E, Moncada S. Induction and potential biological relevance of a Ca(2+)-independent nitric oxide synthase in the myocardium. *Br J Pharmacol*. 1992;105:575–580. doi: 10.1111/j.1476-5381.1992.tb09021.x
29. Palmer RM, Ferrige AG, Moncada S. Nitric oxide release accounts for the biological activity of endothelium-derived relaxing factor. *Nature*. 1987;327:524–526. doi: 10.1038/327524a0
30. Finkel MS, Oddis CV, Jacob TD, Watkins SC, Hattler BG, Simmons RL. Negative inotropic effects of cytokines on the heart mediated by nitric oxide. *Science*. 1992;257:387–389. doi: 10.1126/science.1631560
31. Brunner F, Maier R, Andrew P, Wölkart G, Zechner R, Mayer B. Attenuation of myocardial ischemia/reperfusion injury in mice with myocyte-specific overexpression of endothelial nitric oxide synthase. *Cardiovasc Res*. 2003;57:55–62. doi: 10.1016/S0008-6363(02)00649-1
32. Cameron-Vendrig A, Reheman A, Siraj MA, Xu XR, Wang Y, Lei X, Afroze T, Shikatani E, El-Mounayri O, Noyan H, et al. Glucagon-like peptide 1 receptor activation attenuates platelet aggregation and thrombosis. *Diabetes*. 2016;65:1714–1723. doi: 10.2337/db15-1141
33. Timmers L, Henriques JP, de Kleijn DP, Devries JH, Kemperman H, Steendijk P, Verlaan CW, Kerver M, Piek JJ, Doevendans PA, et al. Exenatide reduces infarct size and improves cardiac function in a porcine model of ischemia and reperfusion injury. *J Am Coll Cardiol*. 2009;53:501–510. doi: 10.1016/j.jacc.2008.10.033
34. Bonnema CF, Zile MR. Pathophysiology of diastolic heart failure: relaxation and stiffness. In: Klein AL, Garcia MJ, eds. *Diastology: Clinical Approach to Diastolic Heart Failure*. 1st ed.; Amsterdam: Elsevier Health Sciences; 2008:11–25.
35. Apstein CS, Grossman W. Opposite initial effects of supply and demand ischemia on left ventricular diastolic compliance: the ischemia-diastolic

paradox. *J Mol Cell Cardiol*. 1987;19:119–128. doi: 10.1016/S0022-2828(87)80551-5
36. Schaefer S, Taylor AL, Lee HR, Niggemann EH, Levine BD, Popma JJ, Mitchell JH, Hillis LD. Effect of increasing heart rate on left ventricular performance in patients with normal cardiac function. *Am J Cardiol*. 1988;61:617–620. doi: 10.1016/0002-9149(88)90776-X
37. Noble MI, Wyler J, Milne EN, Trenchard D, Guz A. Effect of changes in heart rate on left ventricular performance in conscious dogs. *Circ Res*. 1969;24:285–295. doi: 10.1161/01.RES.24.2.285
38. Barragán JM, Rodríguez RE, Blázquez E. Changes in arterial blood pressure and heart rate induced by glucagon-like peptide-1-(7-36) amide in rats. *Am J Physiol*. 1994;266:E459–E466. doi: 10.1152/ajpendo.1994.266.3.e459
39. Yamamoto H, Kishi T, Lee CE, Choi BJ, Fang H, Hollenberg AN, Drucker DJ, Elmquist JK. Glucagon-like peptide-1-responsive catecholamine neurons in the area postrema link peripheral glucagon-like peptide-1 with central autonomic control sites. *J Neurosci*. 2003;23:2939–2946. doi: 10.1523/JNEUROSCI.23-07-02939.2003
40. Griffioen KJ, Wan R, Okun E, Wang X, Lovett-Barr MR, Li Y, Mughal MR, Mendelowitz D, Mattson MP. GLP-1 receptor stimulation depresses heart rate variability and inhibits neurotransmission to cardiac vagal neurons. *Cardiovasc Res*. 2011;89:72–78. doi: 10.1093/cvr/cvq271
41. Ussher JR, Baggio LL, Campbell JE, Mulvihill EE, Kim M, Kabir MG, Cao X, Baranek BM, Stoffers DA, Seeley RJ, et al. Inactivation of the cardiomyocyte glucagon-like peptide-1 receptor (GLP-1R) unmasks cardiomyocyte-independent GLP-1R-mediated cardioprotection. *Mol Metab*. 2014;3:507–517. doi: 10.1016/j.molmet.2014.04.009
42. Reimer KA, Lowe JE, Rasmussen MM, Jennings RB. The wavefront phenomenon of ischemic cell death. 1. Myocardial infarct size vs duration of coronary occlusion in dogs. *Circulation*. 1977;56:786–794. doi: 10.1161/01.CIR.56.5.786
43. Krug A, Mesnil D, de Rochemont KG. Blood supply of the myocardium after temporary coronary occlusion. *Circ Res*. 1966;19:57–62. doi: 10.1161/01.RES.19.1.57
44. Kloner RA, Ganote CE, Jennings RB. The "no-reflow" phenomenon after temporary coronary occlusion in the dog. *J Clin Invest*. 1974;54:1496–1508. doi: 10.1172/JCI107898

Supplemental Material

Data S1.

Supplemental Methods

Metabolic parameters

Myocardial lactate metabolism was calculated as follows:

Venoarterial lactate difference (mmol/L) = coronary sinus lactate (mmol/L) – arterial lactate (mmol/L)

MVO2 is calculated as follows:

MVO2 (mL/min/100 grams) =[(CaO2-CvO2) × CBF]/100 grams heart weight.

Arterial (CaO2) and venous oxygen content (CvO2) were calculated as follows:

CaO2 (mLO2/min/100mL) = [1.34 (mLO2/gram hemoglobin) × hemoglobin concentration (grams/100 mL) × oxygen saturation (%)] + [0.00289 (mLO2/mmHg/100mL) × PaO2 (mmHg)]

and

CvO2 (mLO2/min/100mL) = [1.34 (mLO2/gram hemoglobin) × hemoglobin concentration (grams/100 mL) × oxygen saturation (%)] + [0.00289 (mLO2/mmHg/100mL) × PvO2 (mmHg)].

Coronary vascular resistance (CVR) was calculated as follows:

CVR (mmHg × min/mL/100grams) = aortic mean pressure (mmHg)/coronary blood flow (mL/min)/100 grams heart weight.

Table S1. Perfusate composition in *ex-vivo* heart perfusion before hemoconcentration.

	Dose
Plasmalyte A, mL	450
Mannitol 20%, mL	4
NaHCO3-, mEq	5
Sterile Water, ml	25
Heparin, units	2000
Whole Blood, ml	450
25% Albumin, ml	25
Solumedrol, mg	40

Table S2. Regression results from the linear mixed-effects models of metabolic variables over the course of reperfusion

Myocardial oxygen consumption

Variable	Estimate [95% CI]	p value
Exenatide [ref: control]	-0.189 [-1.420, 1.043]	0.016
Minutes of reperfusion [ref: 30 minutes]		<0.001
60 minutes	0.415 [-0.532, 1.363]	
90 minutes	0.516 [-0.432, 1.463]	
120 minutes	0.541 [-0.459, 1.531]	
Treatment group and minutes of reperfusion interaction		0.008
Treatment group and 60 minutes interaction	1.940 [0.600, 3.280]	
Treatment group and 90 minutes interaction	2.572 [1.232, 3.912]	
Treatment group and 120 minutes interaction	1.771 [0.401, 3.150]	

Venous lactate level

Variable	Estimate [95% CI]	p value
Exenatide [ref: control]	-0.196 [-0.109, 0.064]	0.46
Minutes of reperfusion [ref: 30 minutes]		0.027
60 minutes	0.170 [-0.064, 0.030]	
90 minutes	-0.044 [-0.021, 0.073]	
120 minutes	-0.256 [-0.028, 0.065]	
Treatment group and minutes of reperfusion interaction		0.77
Treatment group and 60 minutes interaction	-0.023 [-0.077, 0.056]	
Treatment group and 90 minutes interaction	-0.066 [-0.118, 0.015]	
Treatment group and 120 minutes interaction	-0.368 [-0.085, 0.047]	

Coronary vascular resistance

Variable	Estimate [95% CI]	p value
Exenatide [ref: control]	-0.023 [-0.109, 0.064]	0.30
Minutes of reperfusion [ref: 30 minutes]		0.36
60 minutes	-0.017 [-0.064, 0.030]	
90 minutes	0.026 [-0.021, 0.073]	
120 minutes	0.018 [-0.028, 0.065]	
Treatment group and minutes of reperfusion interaction		0.51
Treatment group and 60 minutes interaction	-0.010 [-0.077, 0.056]	
Treatment group and 90 minutes interaction	-0.052 [-0.118, 0.015]	
Treatment group and 120 minutes interaction	-0.019 [-0.085, 0.047]	

Figure S1. **Terminal deoxynecleotidyl transferase biotin-dUTP nick end labeling assays.**

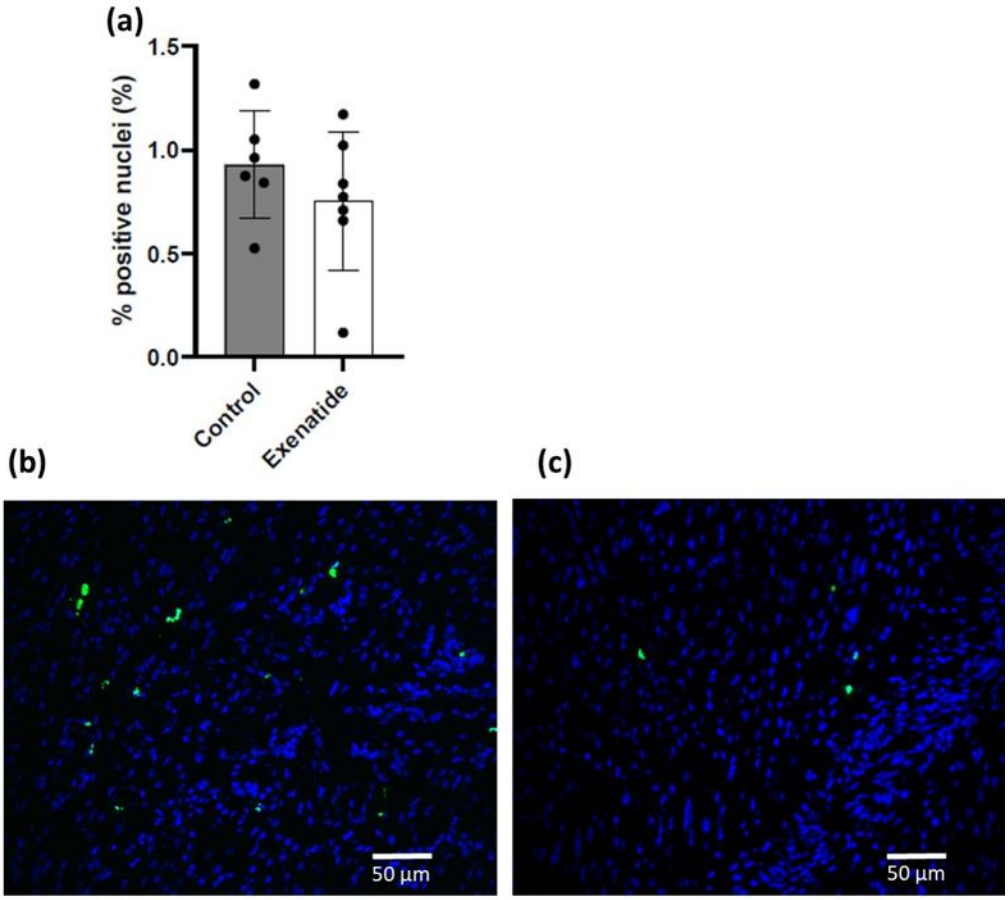

(a) Quantification of % positive nuclei. Representative pictures of stained sections in the control and exenatide group are in (b) and (c), respectively.